Entropically Driven Colloidal Crystallization on Patterned Surfaces

Keng-hui Lin,[1] John C. Crocker,[1,*] Vikram Prasad,[1,†] Andrew Schofield,[2] D. A. Weitz,[1,†]
T. C. Lubensky,[1] and A. G. Yodh[1]

[1]*Department of Physics and Astronomy, University of Pennsylvania, 209 S. 33rd Street, Philadelphia, Pennsylvania 19104-6396*
[2]*Department of Physics and Astronomy, The University of Edinburgh, Edinburgh, United Kingdom EH9 3JZ*
(Received 14 March 2000)

We investigate the self-assembly of colloidal spheres on periodically patterned templates. The surface potentials and the surface phases are induced entropically by the presence of dissolved, nonadsorbing polymers. A rich variety of two-dimensional fluidlike and solidlike phases was observed to form on template potentials with both one- and two-dimensional symmetry. The same methodology was then used to nucleate an oriented single fcc crystal more than 30 layers thick. The general approach provides a new route for directed self-assembly of novel mesoscopic structures.

Colloids self-assemble into a wide range of highly ordered phases. Colloidal crystals form spontaneously in thermal equilibrium [1–3] or can be induced by gravitational [4], convective [5], and electrohydrodynamic [6] forces. These phenomena provide a fascinating test bed for the investigation of many-body statistical physics, and they provide an important paradigm for the creation of three-dimensional photonic structures [7]. In this Letter we demonstrate a novel colloidal system for studies of two-dimensional phase transitions that also provides a qualitatively new approach for colloidal epitaxy based on equilibrium thermodynamics and geometry.

We combine entropic depletion and patterned surfaces with spatially periodic 1D- and 2D-height profiles as templates to influence growth of two- and three-dimensional structures. Depletion effects in suspensions of large and small particles or macromolecules produce forces that push large spheres together [3,8], towards flat walls [9], and towards inner corners on surfaces [10]. We use these forces to attract and repel colloidal spheres from specific positions on a corrugated template.

We observed the formation of 1D, 2D, and 3D commensurate structures as a function of sphere size and grating periodicity. Our experiments complement recent work on charged 2D colloidal phase transitions in a perturbing 1D optical potential [11,12]. Our particle interactions by contrast are short range and are much weaker than the external template potentials, and our surface particle density is set by equilibration at constant chemical potential with the bulk (3D) colloidal liquid. The 1D surface potential induced 2D structures, all of which exhibit diffuse scattering peaks characteristic of 2D bond-angle ordered phases in an aligning field rather than power-law peaks characteristic of 2D crystal order. They thus correspond to the liquid phases of Ref. [12]. In addition, the 2D surface potential induced both liquidlike and solidlike structures and provided the optimum template for growth of a large, defect-free fcc crystal in 3D.

Figure 1 illustrates the depletion force. The Helmholtz free energy of a colloid/polymer mixture decreases by $\Pi \Delta V$ as spheres approach each other. Here Π is the polymer osmotic pressure, and ΔV is the overlap volume, shown in black in Fig. 1A. The free energy reduction at contact at temperature T is $F_0 \approx -2\pi a R_g^2 n_p k_B T$, where a is sphere radius, n_p and R_g are, respectively, the number density and the radius o gyration of the dilute polymer coils [13], and k_B is Boltzmann's constant. Spheres in contact with walls of a grating groove (Fig. 1A) experience an attractive force roughly 4 times the two-sphere value and are forced to the grating "valleys" [10]. Thus the template creates a new class of periodic surface potential for colloidal self-assembly.

Imprint or stamping techniques provide a simple way to make replicas of surface structures [14]. We have employed the imprint technique with an optical diffraction grating to create a geometrical template. We first spincoat a 400 nm thick layer of polymethylmethacrylate (PMMA) on a glass substrate. Pressing a diffraction grating onto the PMMA film (heated above its glass temperature of $\approx 120\,°C$) creates a replica of the grating in the film (Fig. 1B). By rotating the substrate 90° and imprinting a second time, we create two-dimensional periodic structures, resembling an array of square pyramids (Fig. 1C). The templates form one wall of the sealed sample
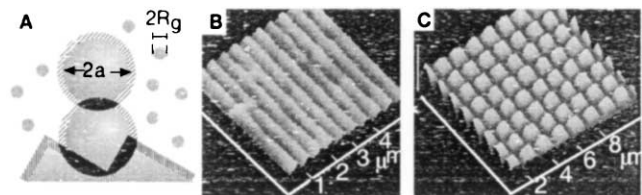

FIG. 1. (A) illustrates the depletion effect. The centers of nonadsorbing polymer coils (small spheres) are excluded from a depletion zone (hashed regions) outside the large spheres and corrugated walls. When these depletion zones overlap (dark shading), the volume accessible to the polymer is increased, increasing polymer-coil entropy and inducing an attractive force between the surfaces. Similarly, spheres are preferentially drawn to interior corners. Atomic force microscope images of (B) the replica optical grating in PMMA and (C) the crossed grating.

chambers which are 30–40 μm thick and contain a few μl of sample.

The colloid samples consisted of 0.7 to 1.2 μm diameter PMMA spheres stabilized by a grafted layer of poly-12-hydroxystearic acid [15,16]. In a mixture of decalin and cyclohexyl bromide, these spheres are nearly density matched and have a refractive index mismatch of <0.01 with respect to the solvent. Such small index mismatches reduce light scattering, facilitating optical microscopy deep into the suspension. Depletion attractions were induced by adding polystyrene with $R_g \approx 15$ nm ($M_w = 320\,000$, $M_w/M_n = 1.04$, Polymer Laboratories). We adjusted polymer concentration to keep F_0 fairly constant as we varied the spatial period p of the template and the sphere size. 2D surface structures formed approximately in one hour and evolved very slowly thereafter. They exhibited local density inhomogeneities and defects whose positions were quenched over the lifetime of the experiments.

The interplay between bulk particle volume fraction, Φ, bulk polymer concentration, C_P, and mean nearest-neighbor spacing, d, on the surface is most clearly exhibited by the 1D colloidal liquids that form in the grooves of the 1D grating template. The simplest case arises when the spheres are large enough to fill the groove, but not large enough to interact with spheres in adjacent grooves. Our observations for self-assembly on the line gratings are displayed along with the corresponding structure function, $S(\mathbf{k})$, in Fig. 2. The 1D liquid phase (i.e., stripe phase) is shown in Fig. 2A, and its pair correlation function along the groove, $g(r)$, is plotted in Fig. 3A for three different combinations of Φ and C_P. We derived an approximate bulk phase diagram for this system based on [16] (see the inset in Fig. 3). At low volume fraction Φ, the measured pair correlation function $g(r)$ exhibited peaks whose positions were identical to and whose asymmetric shapes were similar to those of a classical hard-core gas [17]; its magnitude, however, decayed more rapidly toward 1 at large r than a hard core gas. At higher concentrations the mean nearest-neighbor spacing, d, derived from the first peak in $g(r)$, shifted to smaller values, but the typical spacing was larger than the depletion interaction range, about 1.1 diameter. These observations suggest that the surface density of spheres is determined by the competition of the depletion attractions driving the spheres to the surface and the osmotic pressure of the spheres already there.

When the sphere diameter increases relative to the grating period p, the 1D colloidal liquids in adjacent rows interact more strongly. The most important parameter characterizing the 2D phase behavior is the commensurability ratio, $\chi = d/p$, where d is derived from the pair correlation function along the groove. For the phases in Fig. 2, $\Phi = 0.25$ is high enough to serve as a reservoir for surface adsorption. C_P was set near the *bulk* fluid-crystal phase transition region (point "X" in Fig. 3 [16]). This choice ensured that bulk crystallization did not occur in our thin sample chambers and that the spheres densely cover
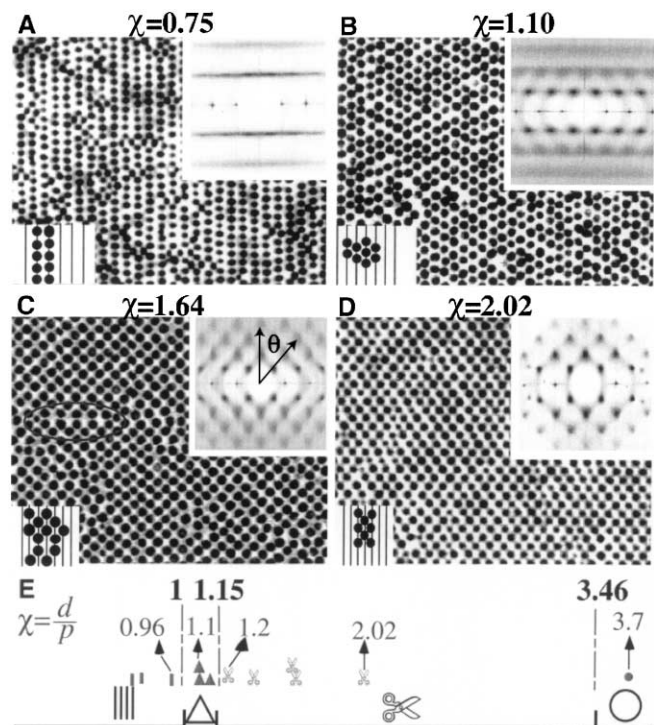

FIG. 2. Phase-contrast micrographs of four representative 2D structures with the schematic reconstruction in the bottom left corner. The $S(k)$ computed from these images is shown in the top right corner. (A) Stripe phase. (B) Triangular phase. (C),(D) Scissor (centered-rectangular) phases with different scissor angles as defined in the structure function image of (C). In (C) we circle the mirror line of a twinning defect. (E) Diagram indicating the observed phases as a function of χ.

the template surface. On flat substrates, the colloid formed isotropic liquid structures at these same concentrations. The line grating breaks symmetry in one direction, and the assembled structures exhibit a range of two-dimensional patterns. Generally, the 2D colloidal structures on the line-grating surfaces do not exhibit very long-range translational order along the groove direction. Point defects and dislocations are common, as are twinning planes perpendicular to the groove direction (see Fig. 2C).

Hexagonal symmetry emerges in 2D through the interlacing of spheres in different grooves for $1 < \chi < 2/\sqrt{3} = 1.15$ (see Fig. 2B). As χ increases towards 1.15, this structure becomes more ordered, and for $1.15 < \chi < 2\sqrt{3} = 3.46$, the ordered structure is maintained while hexagonal symmetry gives way to crystals with centered rectangular unit cells (see Figs. 2C and 2D). 2D phases with centered rectangular symmetry have not been previously observed [11]. We define the scissor angle, θ, as the angle between the grating groove direction and the crystal lattice vector (see Fig. 2C) and refer to the centered rectangular phase as the scissor phase. Using the geometric relation $\tan\theta = 2p/d$, we again find that the mean nearest-neighbor spacing is $\approx 10\%$ bigger than the sphere diameter.
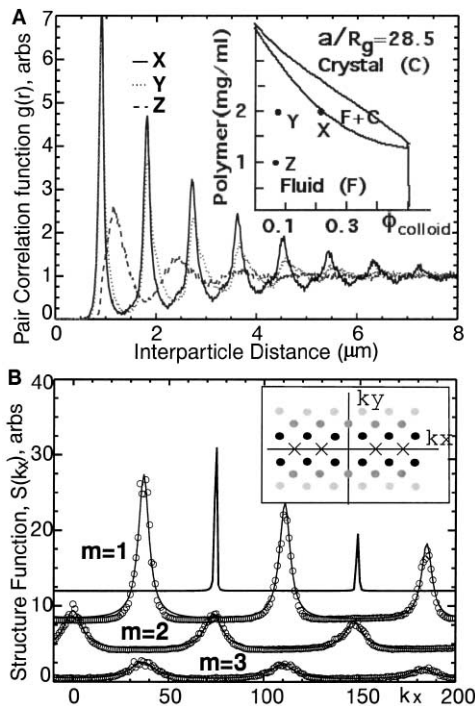
FIG. 3. (A) 1D pair correlation function along the groove direction for colloidal spheres in the stripe phase ($2a = 0.86\ \mu$m, $p = 1.21\ \mu$m; see Fig. 2A). For curve X, the first peak of $g(r)$ occurs at $r = 0.93\ \mu$m. The inset is the approximate bulk phase diagram scaled from [16] for this system as a function of Φ and C_P. (B) $S(k)$ for the centered rectangular phase shown in Fig. 2C. The peak positions are indicated in the inset. The $\times$'s indicate delta-function Bragg peaks and circles indicate Lorentzian-like peaks. The grooves are aligned parallel to the Y axis and plot $S(k)$ vs k_x, at four different values of k_y. The topmost row shows the Bragg peaks (i.e., at $k_y = 0$) scaled $50\times$ smaller. For nonzero k_y, the curves are well modeled by Eq. (1) (solid curves).

To understand better the nature of these phases, we examined the shape of the peaks in the structure function, $S(\mathbf{k})$. It exhibits resolution-limited Bragg peaks, arising from the periodic template, at $k_y = 0$ and $k_x = nG_x$, where $G_x = 2\pi/p$ and n is an integer, and diffuse peaks along the lines $k_y = mG_y$ with m an integer, where $G_y = 2\pi/d$, reflecting correlations within and between grooves. The intensities as a function of k_x at $k_y = mG_y$ are well described for all $m \neq 0$ and χ by

$$S_m(k_x) = \frac{A_m e^{-k_x^2 W_m}}{1 + C_m \cos(k_x p)} + B_m, \tag{1}$$

which exhibits Lorentzian peaks of width squared $2(1 - |C_m|)/p^2|C_m|$ at k_x equal to odd multiples of $G_x/2$ for $C_m > 0$ and to even multiples of $G_x/2$ for $C_m < 0$. This is the scattering function for a model system in which a 1D liquid in each groove interacts weakly with the liquids in its nearest-neighbor grooves. Within this model, W_m is a Debye-Waller factor arising from uncorrelated motion of spheres perpendicular to the grooves, C_m is proportional to the product of the interparticle potential at wave number $k_y = mG_y$ and

the structure factor $S_{1D}(mG_y)$ of the spheres along an isolated groove, A_m is an amplitude proportional to $S_{1D}(mG_y)$, and B_m is a background. In the stripe phase, there is short-range simple rectangular order (see Fig. 2A), and $S_m(k_x)$ exhibits diffuse peaks at $k_x = nG_x$ for $m = 1$ and $m = 2$ described by Eq. (1) with $C_m < 0$, corresponding to attractive interactions between spheres in neighboring grooves. The ratio C_1/C_2 is equal within experimental error to $S_{1D}(G_y)/S_{1D}(2G_y)$ determined by direct measurement of the 1D structure function of a line, in agreement with the model of weakly interacting 1D liquids. As the density is increased, centered-rectangular (or hexagonal) correlations become more pronounced, and the structure function peaks become those of a centered rectangular reciprocal lattice at $k_x = (n + \frac{1}{2})G_x$ for m odd and $k_x = nG_x$ for m even. We observe this effect in the scissor and hexagonal phases, whose structure functions are well described by Eq. (1) (even though the intergroove coupling is no longer weak) with $C_m > 0$ for m odd and $C_m < 0$ for m even. A similar structure function results when unbound or quenched dislocations convert the power-law Bragg peaks of the "locked floating solid" phase of Ref. [12] to Lorentzian peaks in the liquid phase. In our experiments, W_n was approximately constant, and $|C_m|$ decreased with increasing m in all phases. The decay of $|C_m|$ was slower in the scissor phase than in the hexagonal phase.

The crossed gratings impose a 2D external potential. Since the crossed grating has two-dimensional square symmetry, we expect the assembled structures to have this symmetry. All the ordered patterns have square symmetry, but with different lattice constants and orientation (see Fig. 4). Here $d = 1/\sqrt{\sigma}$, where σ is the particle surface density. When $\chi \sim 1/\sqrt{2} \approx 0.71$, a commensurate overlay fcc(100) $1/\sqrt{2} \times 1/\sqrt{2}$ 45° formed. When $\chi \sim 1$, commensurate structures with fcc(100) 1×1 pattern were formed, and finally for $\chi \approx \sqrt{2} = 1.41$, a commensurate, rotated square structure formed, i.e., fcc(100) $\sqrt{2} \times \sqrt{2}$ 45°. In the latter case large domains did not arise because two possible nucleation sites exist on the template and produce different lattices, corresponding to lattices built on either the black or the white squares of a checkerboard. When d was commensurate with the pitch at the ratios 0.71, 1, and 1.41, larger crystal domains with fewer defects formed.

The structure functions for crossed-grating phases had both solidlike and liquidlike features. Each phase exhibited Bragg-like peaks on the reciprocal lattice of the template potential along with a ringlike background and diffuse peaks characteristic of a liquid or residual sample disorder. Generally the diffuse peaks were narrower than the corresponding peaks in the 1D potential. When χ deviates from the commensurate values, the liquidlike ring becomes more pronounced.

Finally, a crossed grating commensurate with the fcc(100) plane ($\chi = 1$) was used to grow an fcc crystal
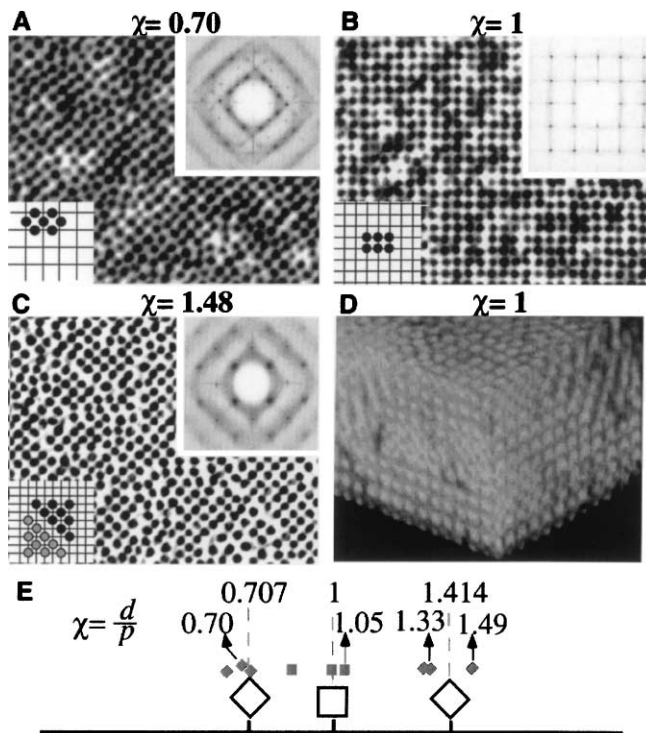
FIG. 4.   (A), (B), and (C) illustrate 2D colloidal assembly commensurate with the crossed-grating template. Notice that the crystal orientation rotates by 45 degrees for $\chi = 0.71$, 1.41, and that different crystal domains are clearly seen in (C). The domain size in (B) is greater than the microscope field of view which is 60 μm $\times$ 80 μm. (D) 3D confocal image showing 20 layers within the interior of a > 30 layer fcc crystal grown with no density match on the template as in (B).

without stacking defects (Fig. 4D). With some density mismatching (e.g., 0.3 g/cm^3 difference), the growth process was enhanced by a gravity-induced increase in sphere concentration near the surface; then the spheres crystallized faster and grew more than 30 layers. In contrast to previous sedimentation-based assembly [4], control experiments without polymer did not produce large ordered colloidal crystals probably because the energy difference between the top and the bottom of the groove is only $0.2 k_B T$ (3$\times$ less than [4] and 20$\times$ less than with the depletion effect). Nevertheless, after >24 h, a few layers of crystal nucleated.

To conclude, we have reported on a rich variety of 2D self-assembly phenomena using mixtures of colloids, polymers, and entropic surface potentials. Moreover, the combination of depletion attraction and a simple, robust surface templating scheme provides a qualitatively new route for controlled colloidal self-assembly in 3D. Since the entropic techniques used here are not restricted to micron size particles, the underlying principles should be applicable on smaller, macromolecular length scales.

---

*Present address: Applied Physics Department, California Institute of Technology, Pasadena, CA 91125.

†Present address: Physics Department and DEAS, Harvard University, Cambridge, MA 02138.

[1] A. D. Dinsmore, J. C. Crocker, and A. G. Yodh, Curr. Opin. Colloid Interface Sci. **3**, 5 (1998).

[2] A. P. Gast and W. B. Russel, Phys. Today **51**, No. 12, 24 (1998).

[3] P. N. Pusey and W. van Megan, Nature (London) **320**, 340 (1986); B. J. Ackerson and P. N. Pusey, Phys. Rev. Lett. **61**, 1033 (1988).

[4] A. van Blaaderen, R. Ruel, and P. Wiltzius, Nature (London) **385**, 321 (1997).

[5] R. Micheletto, H. Fukuda, and M. Ohtsu, Langmuir **11**, 3333 (1995); N. D. Denkov et al., Nature (London) **361**, 26 (1993); I. Peterson, Science **148**, 296 (1995); P. Kralchevsky and K. Nagayama, Langmuir **1**, 23 (1994).

[6] M. Holgado et al., Langmuir **15**, 4701 (1999).

[7] I. I. Tarhan and G. H. Watson, Phys. Rev. Lett. **76**, 315 (1996); A. Imhof and D. J. Pine, Nature (London) **389**, 948 (1997); J. E. G. J. Wijnhoven and W. L. Vos, Science **281**, 802 (1998); O. D. Velev et al., Nature (London) **401**, 548 (1999); A. Y. Vlasov, N. Yao, and D. J. Norris, Adv. Mater. **11**, 165 (1999); G. Subramania et al., Appl. Phys. Lett. **74**, 3933 (1999); E. Yablonovitch, Nature (London) **401**, 539 (1999).

[8] J. S. Duijneveldt, A. W. Heinen, and H. N. W. Lekkerkerker, Europhys. Lett. **21**, 369 (1993); A. D. Dinsmore, A. G. Yodh, and D. J. Pine, Phys. Rev. E **52**, 4045–4057 (1995); A. Imhof and J. K. G. Dhont, Phys. Rev. Lett. **75**, 1662 (1995).

[9] P. D. Kaplan, J. L. Rouke, A. G. Yodh, and D. J. Pine, Phys. Rev. Lett. **72**, 582 (1994); A. D. Dinsmore et al., Phys. Rev. Lett. **80**, 309 (1998).

[10] A. D. Dinsmore and A. G. Yodh, Langmuir **15**, 314 (1999); A. D. Dinsmore, A. G. Yodh, and D. J. Pine, Nature (London) **383**, 239 (1996).

[11] A. Chowdhury, B. J. Ackerson, and N. A. Clark, Phys. Rev. Lett. **55**, 833 (1985); Q.-H. Wei, C. Bechinger, D. Rudhardt, and P. Leiderer, Phys. Rev. Lett. **81**, 2606 (1998).

[12] E. Frey, D. R. Nelson, and L. Radzihovsky, Phys. Rev. Lett. **83**, 2977 (1999).

[13] S. Asakura and F. Oosawa, J. Polym. Sci. **32**, 183 (1958); A. Vrij, Pre. Appl. Chem. **48**, 471 (1976).

[14] S. Y. Chou et al., J. Vac. Sci. Technol. B **15**, 2897 (1997); Y. Xia et al., Science **273**, 347 (1996).

[15] L. Antl et al., Colloids Surf. **17**, 67 (1986).

[16] S. M. Ilett, A. Orrock, W. C. K. Poon, and P. N. Pusey, Phys. Rev. E **51**, 1344 (1995).

[17] E. H. Leib and D. C. Mattis, *Mathematical Physics in One Dimension* (Academic Press, New York, 1966).